Analysis of Parachute Opening Dynamics with Supporting Wind-Tunnel Experiments

H. G. HEINRICH* AND R. A. NOREEN†
University of Minnesota, Minneapolis, Minn.

The equation of motion for parachutes inflating under finite mass conditions in a horizontal flow wind tunnel is established and organized in view of the nonsteady terms of canopy size, velocity, included and apparent masses, and the time derivatives of these terms. Wind-tunnel experiments are described, the results of which yield graphical and numerical time functions for the terms of the equation of motion. In the test range under investigation, these functions appear to be unique. The wind-tunnel results are compared with full-size test information and certain identities are shown. The numerical functions are substituted in the equation of motion and force-time histories calculated. Calculated and measured forces agree fairly well, and the calculations show the contributions of the various terms to the total force.

Nomenclature

C_D = drag coefficient
c = effective porosity
D = drag, diam
F = force
h = altitude
K' = constant determined by the shape of the body
m = mass
R = radius
S = area
T = dimensionless filling time, t/t_f
t = time
V = volume
V_0 = measured canopy included volume at steady state, 1.97 ft^3
v = velocity
W = weight
ρ = density

Subscripts

a = apparent
f = filling
g = gravity
i = included
0 = nominal
p = parachute, projected
s = suspended, snatch when used with velocity
W = wind tunnel

I. Introduction

THE best known and most analytically oriented methods to calculate parachute opening forces,[1-3] incorporate terms derived from theoretical considerations and from experimental evidence obtained from full-size field tests or from wind-tunnel measurements. They also include certain assumptions and simplifications. For example, the drag coefficients utilized are from steady-state wind-tunnel measurements, the variation of parachute shapes during the period of inflation follows a certain scheme,[2] and the rate of growth of the canopy's drag area is assumed to be constant.[3] However, in particular, the method in Ref. 3 is very frequently used and provides values for the maximum force satisfactory for design layouts.[4]

In full size tests, a unique size-time function was found, which was independent of velocity and altitude when related to the dimensionless time T.[5,6]

If this unique function can be verified over a wide range of application, it could be introduced in the method under Ref. 3 and would probably lead to a considerable improvement of this opening force calculation method.

In the following study, the size-time, velocity-time, and volume-time histories of the equation of motion have been measured in wind-tunnel experiments under the condition of a finite suspended mass. These terms were measured for three different velocities, they showed a relatively mild ve-

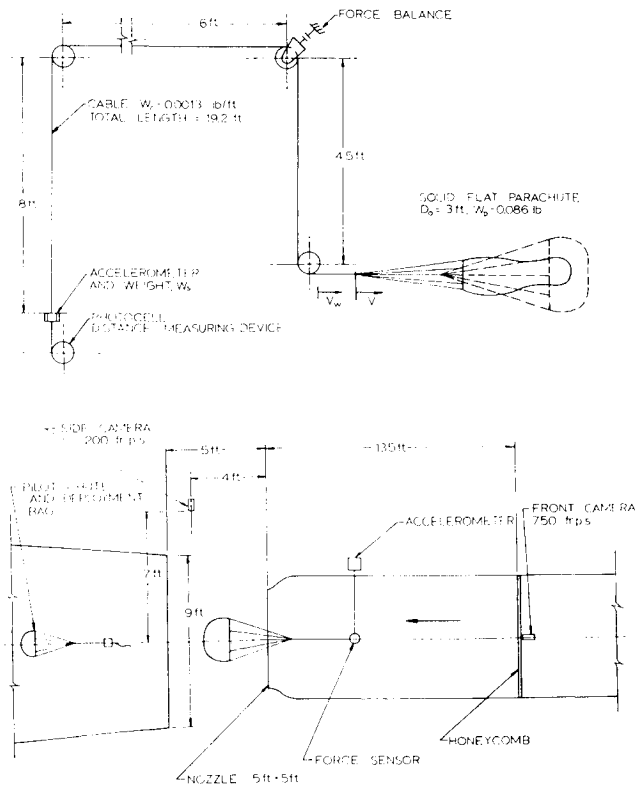

Fig. 1 Wind-tunnel arrangement for testing under finite mass condition.

Presented as Paper 68-924 at the AIAA 2nd Aerodynamics Deceleration Systems Conference, El Centero, Calif., September 23-25, 1968; submitted October 29, 1969; revision recieved December 24, 1969. This study was sponsored by U. S. Air Force Contract No. F33615-67-C-1010.

* Professor, Institute of Technology, Department of Aeronautics and Engineering Mechanics. Fellow AIAA.

† Scientist, Institute of Technology, Department of Aeronautics and Engineering Mechanics. Associate Member AIAA.

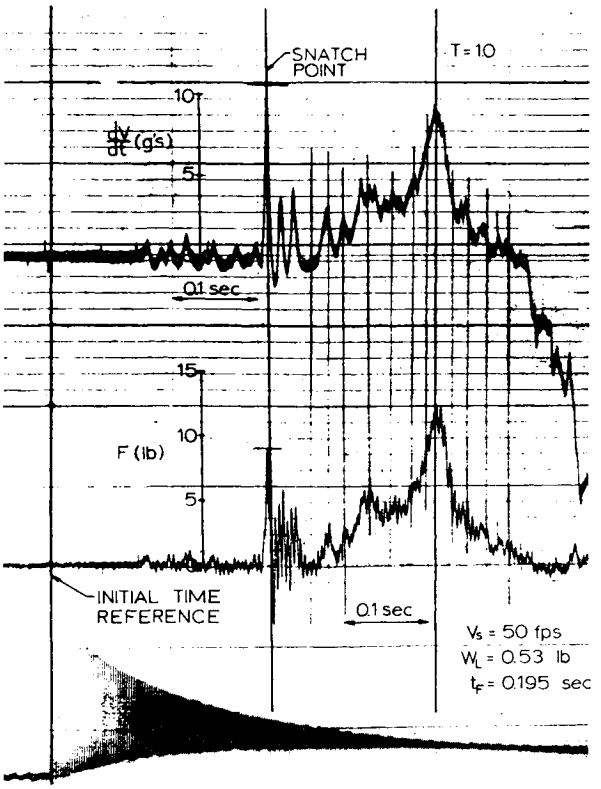

Fig. 2. Typical oscillograph recording of finite mass test system.

locity dependency, and their combination to average relationships appeared to be justified. This size-time history was compared with the one obtained from field tests.[5,6] Certain deviations were noticed in the early phase of inflation while towards the end of the inflation process the agreement between model and full-size tests is fairly good. More recent tests with much more flexible models have shown a better agreement of size-time histories between model and full-size tests, and the observed deviation can be attributed to model stiffness.

In the same manner, average velocity-time and volume-time histories were established. Numerical functions were derived for all averaged relationships. These functions were introduced into the equation of motion, and the force-time relationships were calculated. The calculated forces agreed reasonably well with measured model forces, and it appears that the noted velocity dependency of these otherwise unique functions is small enough to permit utilization of these average functions for force calculations. Also, the force calculations illustrate nicely the contributions of the various terms to the total force. For example, it is interesting to note that the effects of the included and apparent masses provide very significant contributions.

II. Equation of Motion

For the study of the model parachute inflation under finite mass conditions, a wind-tunnel test system was arranged as shown in Fig. 1.

For the deployment of a parachute in a wind tunnel and using the illustrated arrangement, the equation of motion amounts to

$$(d/dt)[(m_s + m_p + m_i)V] = D - W_s + F_a + V_W(dm_i/dt) \quad (1)$$

where F_a is the force because of the apparent mass effect, and $V_W(dm_i/dt)$ represents the momentum of the air trapped in

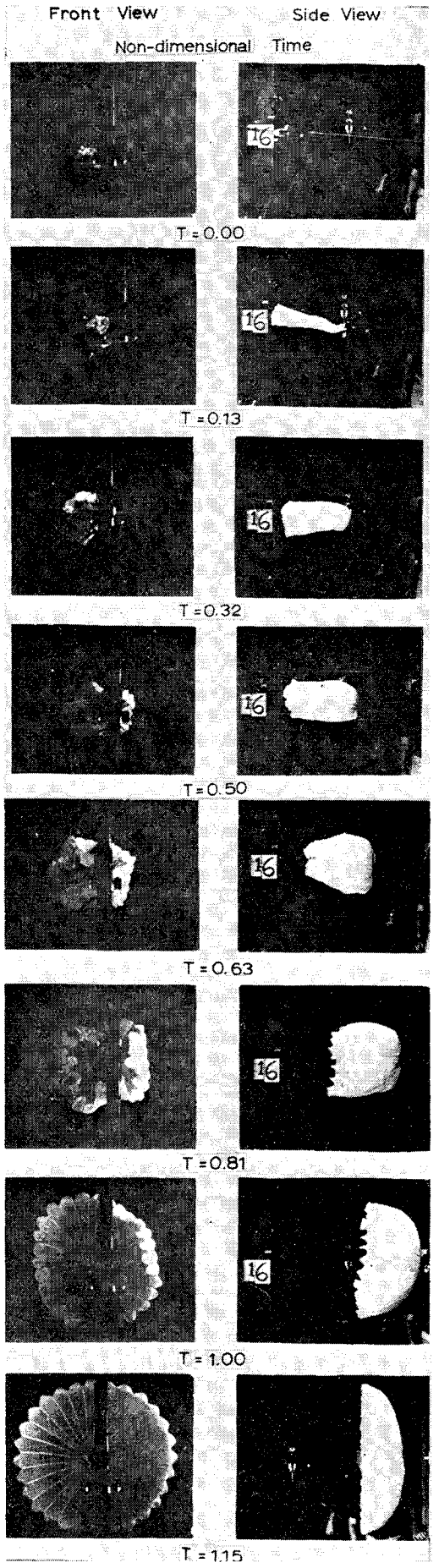

Fig. 3 Typical opening sequence of a 3-ft solid flat cloth parachute.

the canopy due to the relative velocity between the parachute and the air in the wind tunnel. Using for the wind tunnel and system velocities V_W and V, respectively, and expressing F_a as

$$F_a = (d/dt)[m_a(V_W - V)] \tag{2}$$

the equation of motion can be written

$$m_s(dV/dt) = \tfrac{1}{2}\rho C_D S(V_W - V)^2 - W_s + (V_W - V)[(dm_i/dt) + (dm_a/dt)] - (m_p + m_i + m_a)(dV/dt) \tag{3}$$

The system velocity V, is positive in the direction of the drag vector and because of the experimental arrangement, dV/dt is by definition always positive. With these terms, the force upon the suspended weight amounts to

$$F = m_s(dV/dt) + W_s = \tfrac{1}{2}\rho C_D S(V_W - V)^2 + (V_W - V)[(dm_i/dt) + (dm_a/dt)] - (m_p + m_i + m_a)(dV/dt) \tag{4}$$

An inspection of the right-hand side of Eq. (4) shows the nonsteady terms of the systems velocity V, the area S, the included mass m_i, the apparent mass m_a, and the time derivatives of these terms. The equation also includes the drag coefficient C_D which for the purpose of this study, was obtained from steady-state wind-tunnel tests on simulated canopy shapes. Unfortunately, the respective drag coefficients of parachutes during the nonsteady process of inflation are so far not available.

III. Experimental Arrangement and Test Conditions

As shown in Fig. 1, the parachute model is connected by means of a cable and pulley system to a weight. During the tests, the model parachute is initially packed in a deployment bag and held at a particular point. The bag is connected to a pilot parachute, which, when released, accelerates the bag and removes it from the canopy when the suspension lines of the model are fully extended. At this instance, the snatch force occurs, and thereafter the canopy begins to inflate. The deployed parachute pulls at the suspended weight, lifts it up, and the canopy moves downstream.

In order to determine the nonsteady terms, the force between parachute and suspended weight was measured by means of a strain gage balance, the acceleration sensed by an accelerometer, and the velocity of the suspended weight was recorded by means of a rotating slotted disk and a photocell arrangement. The outputs of the sensor for the force F, the acceleration dV/dt, and the system velocity V, were recorded on an oscillograph. In order to establish the rate of growth of the canopy and to derive the included and apparent mass terms, movie cameras for side and frontal views were used as indicated in Fig. 1. A typical recording diagram is shown in Fig. 2 while Fig. 3 shows sequence pictures of the inflating parachute model.

The parachute model was geometrically similar to a 28-ft standard flat circular parachute, and its nominal diameter was 3 ft. In order to keep the model as flexible as possible, the suspension lines ended at the canopy skirt and were woven nylon lines with a breaking strength of 10 lb. A calculation showed that for these experiments the stress strain characteristics of parachute cloth and lines were insignificant for the force development. The suspended weight W_s consisted of an accelerometer with a range of ± 50 g and an additional weight. The accelerometer and weight amounted to 0.53 lb, which in connection with the canopy surface area yields a surface loading W_s/S_0 of 0.075 lb/ft^2.

In view of the wind tunnel and instrumentation capability, initial velocities of 50, 70, and 85 fps were chosen, and in view of the test arrangement, these speeds are the snatch velocities of the model parachutes.

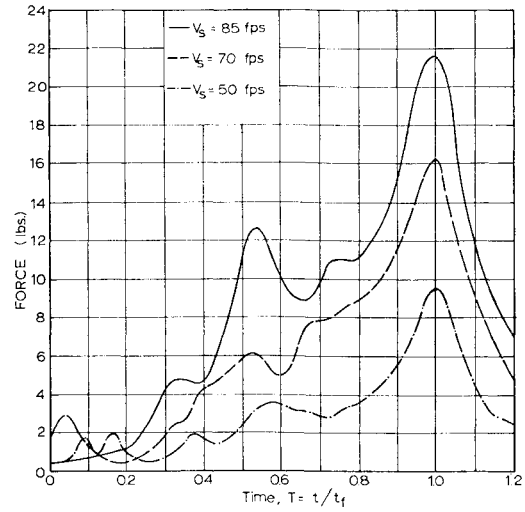

Fig. 4 Averaged force-time histories at V_s = 50, 70, 85 fps.

The surface loading of a man carrying parachute under steady-state descent is in the order of 0.325 lb/ft^2. It was not advisable to experiment with the higher-surface loading since respective tests yielded oscillograms looking like force recordings of parachute inflations under infinite mass conditions. With more sophisticated instrumentation, it may have been possible to interpret them properly. Also it appears that parachute model tests duplicating the characteristic opening dynamics do not necessarily need to be made with identical surface loadings. Ideally all terms in the equations of motion of full size and model parachute should have the same ratio in order to provide perfect dynamic similarities. Reviewing the dynamic equation, one notices that besides the surface loading, other powerful terms are involved, for example, as the sum of the included and apparent masses and their time derivatives. With the selected test conditions, the ratios of included to suspended masses of the model and a 28-ft flat circular parachute differed merely by a factor of two under sea level conditions and approached unity for the full-size parachute at 20,000-ft altitude. Therefore, the concept of these tests favors more the similarity of the mass ratios than the surface loadings.

IV. Model Force-Time Histories

The test results to be looked at first are of course the force-time histories measured by the strain gage device shown in Fig. 1. The indicated forces were corrected for the masses and moments of inertia of the pulleys and cables involved. A considerable number of experiments at the three velocities were made, and the results of all valid tests have been composed to average force-time histories as shown in Fig. 4. As general characteristics, one notices that the peak force increases with snatch velocity, that each diagram shows an early force increase, and a period of somewhat steady or reduced force before the rise to the final peak. This general behavior was also shown by Berndt,[5] who evaluated and averaged full-size drop tests; and Fig. 5 indicates typical differences between the force-time relationships of two experiments at the same altitude and approximately the same snatch velocity.[7] Comparing the force-time histories of the individual runs of the wind-tunnel experiments, one finds that the variation in force recordings in wind-tunnel and in full-size experiments is of about the same order.

For the final comparison between wind-tunnel results, Fig. 4, and recordings available from full-sized tests, three full-size force recordings have been chosen with maximum forces which agree with those given as characteristic values in Refs. 5 and 6.

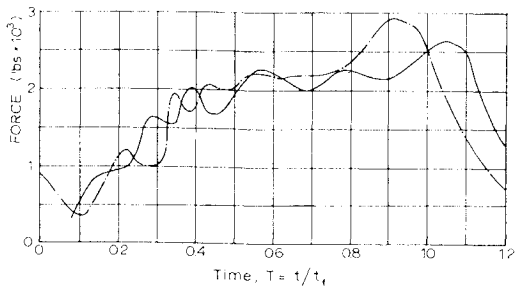

Fig. 5 Force-time histories of 28-ft solid flat parachutes at $V_s \approx 230$ fps and $h = 13{,}000$ ft.

These are also experiments in which the ratios of included and apparent masses to the suspended mass are very close to those of the wind-tunnel studies. These full-size tests include also possible effects of varying effective porosity,[7] but no effort has been made to eliminate these influences from these characteristics. Comparing then Figs. 4 and 6, one notices a general similarity between wind-tunnel and full-sized experiments, particularly with those conducted at 20,000-ft altitude, where the mass ratios are closest. In summary, the wind-tunnel experiments compare with individual and average force-time histories of full-size parachutes well enough so that the evaluation of the wind-tunnel tests in view of an analysis of the opening dynamics is justified.

V. Nonsteady Terms and Their Combinations

Besides the force measurement, the two directly measured nonsteady terms appearing on the right-hand side of the equation of motion are the acceleration of the suspended weight and its velocity. The recorded acceleration was used as a cross check on the measured forces and velocities. Data points and an averaged curve for one velocity are shown in Fig. 7. The spread of data points shown is typical for all experimentally established nonsteady terms. The velocity-time histories showed a slight dependency on snatch velocity (Fig. 8). However, for the purpose of this study, these deviations appear small and an average curve was computed (Fig. 9) for which, by means of a curve fitting process, the function below was established. This function will be used in all further calculations.

$$V/V_s = [1.774 - (T - 0.065)^2]^{1/2} - 0.33$$

for $0 < T < 1.0$

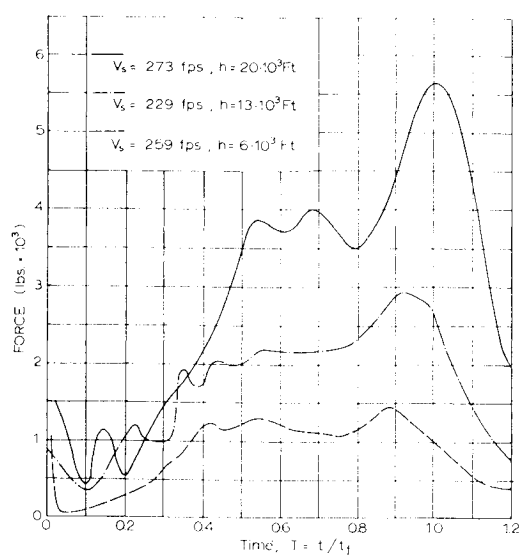

Fig. 6 Characteristic force-time histories of 28-ft solid flat parachutes at nearly constant speed but different altitudes.

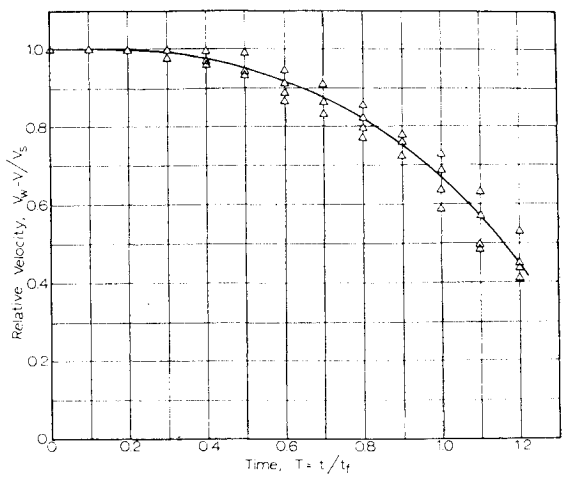

Fig. 7 Relative velocity of model parachute at snatch velocity of 70 fps.

and

$$V/V_s = 0.958 - [0.332 - (T - 1.463)^2]^{1/2} \qquad (5)$$

for $1 < T < 1.4$.

The next two important nonsteady terms are the canopy projected area and the included mass. Both were obtained from the high speed motion pictures for a considerable number of tests made at the speeds of 50, 70, and 85 fps. The generalized size-time histories of the canopy projected area under the various test conditions are shown in Fig. 10. Again, the curves were combined to an average curve (Fig. 11). For comparison, the generalized curves from Refs. 5 and 6 are also marked in Fig. 11. One observes a good agreement at the higher values but some deviation for lower filling time values. It appears that the relatively higher stiffness of the parachute model causes this deviation, because later tests with a much more flexible and lighter model showed a better agreement with the respective curves of full-size tests.

From the averaged size-time curve, the radius of an imaginary circular disk was computed and approximated by a function (Fig. 12) which can be arranged in the form of

$$R_p/R_0 = 0.097 + 0.471\ T \text{ for } 0 < T < 0.8$$
$$R_p/R_0 = 1.4 - 2.8\ T + 2.05\ T^2 \text{ for } 0.8 \leq T \leq 1.0 \qquad (6)$$
$$R_p/R_0 = 0.475 + [0.091 - (T - 1.245)^2]^{1/2}$$

for $1.0 < T < 1.3$.

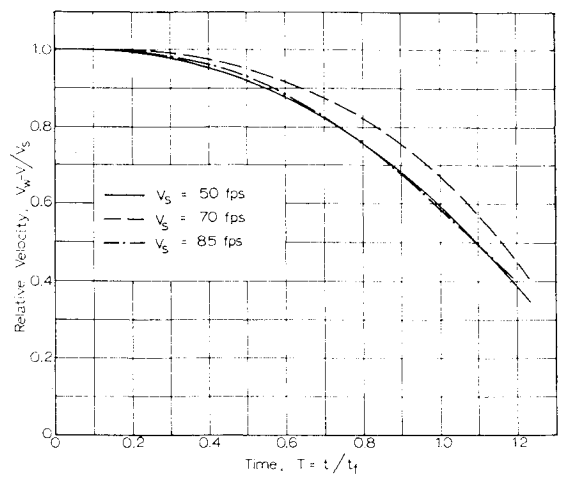

Fig. 8 Ratio of relative velocities of the model parachute at 50, 70, and 85 fps.

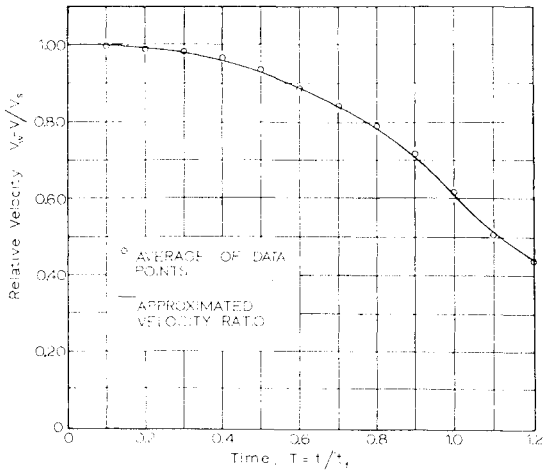

Fig. 9 Approximated velocity ratio vs time.

A second evaluation of the film recordings yielded the volume inclosed by the inflating canopy. With the assumption of constant air density, the volume-time curve also represents the included mass-time history. Utilizing a film evaluation similar to the determination of the instantaneous projected area, contours of the canopy were obtained and were approximated by hemispheres, semiellipses, and truncated cones. The volume of these replacement bodies provided an approximation of the instantaneous canopy inclosed volume. Again, a number of experiments was evaluated and the individual results were generalized with respect to a canopy volume at steady-state conditions and filling time of the individual runs. The results of these measurements and an averaged curve representing the volume-time history is shown in Fig. 13. For the evaluation of the equation of motion, the averaged volume-time history was approximated by four functions yielding the equations, their derivatives, and the approximate curve in Fig. 13.

For $0 \leq T < 0.7$,

$$V/V_0 = 0.185\ T + 0.427\ T^2 - 0.139\ T^3 \qquad (7)$$

and for $0.7 \leq T \leq 1.0$,

$$V/V_0 = -1.28 + 41.48\ T - 83.25\ T^2 + 75.18\ T^3 - 25.4\ T^4 + 50.8(T - 0.6)^5 + 2540(T - 0.75)^8 \qquad (8)$$

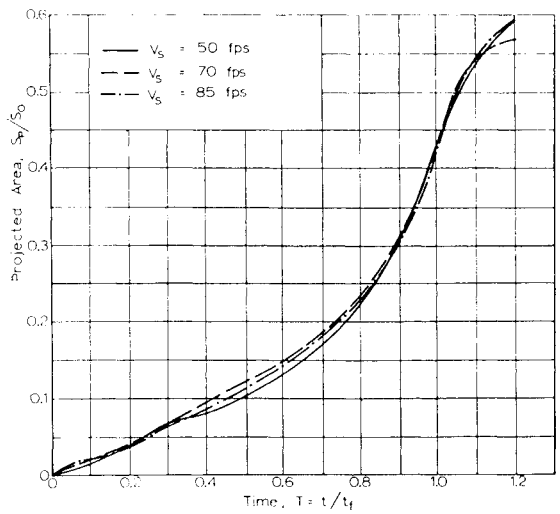

Fig. 10 Canopy projected area ratios at snatch velocities of 50, 70, and 85 fps.

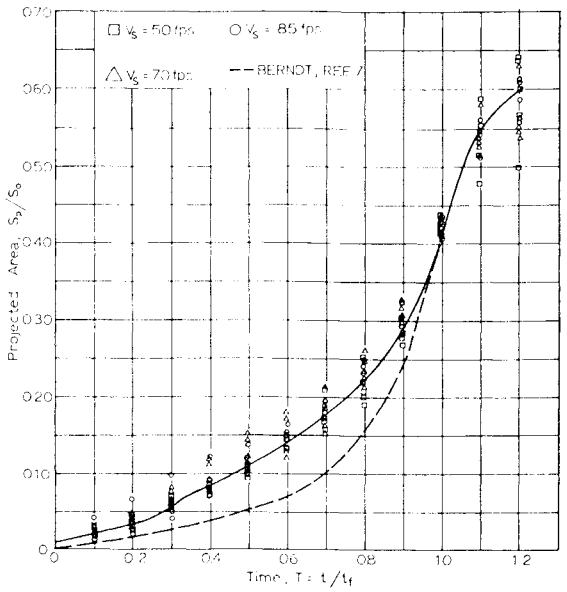

Fig. 11 Ratio of projected and total canopy area vs time.

and for $1.0 < T \leq 1.07$,

$$V/V_0 = 0.98 + 1.27[0.0123 - (T - 1.12)^2]^{1/2} \qquad (9)$$

and for $1.07 < T \leq 1.20$,

$$V/V_0 = 0.881 + 1.27[0.0437 - (T - 1.18)^2]^{1/2} \qquad (10)$$

The equation of motion also includes the apparent mass and its time derivative. In classical literature, theoretical treatments of the apparent mass for a number of basic bodies such as circular disks, ellipsoids, and spheres can be found. More recently Ibrahim[9] calculated for potential flow the apparent mass of nonporous hemispherical shells, and determined it experimentally for perforated rigid cups simulating ribbon parachutes. Earlier, Ref. 10, the apparent mass of actual parachute canopies was measured yielding the

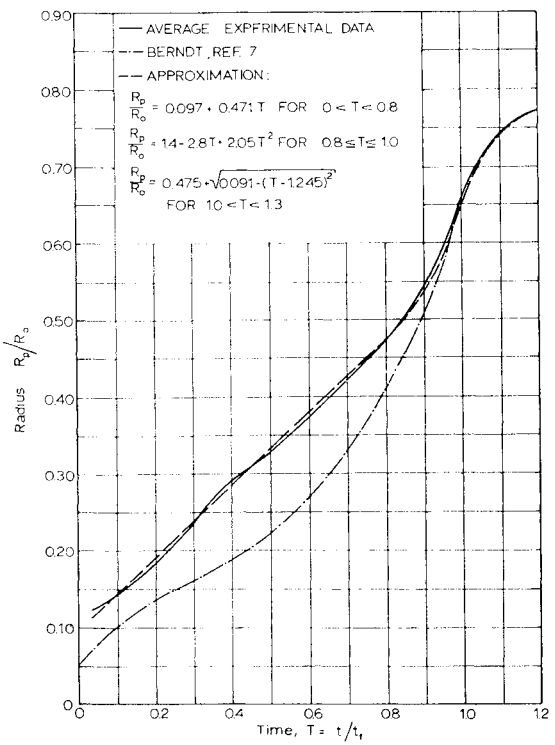

Fig. 12 Averaged and approximated radius ratio vs time.

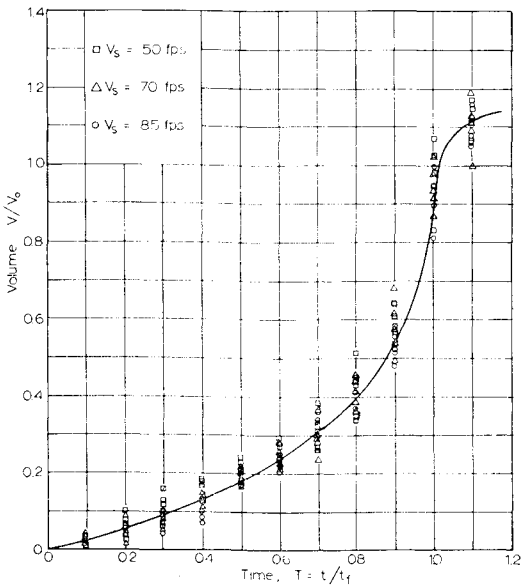

Fig. 13 Ratio of instantaneous to steady-state canopy volume vs dimensionless time T.

relationship

$$m_a = K'\pi R^3\rho \tag{11}$$

in which the constant K' depends on the shape and porosity of the parachute canopy. It was shown that for solid flat parachutes with an effective porosity of $C = 0.05$,[8] the constant amounts to $K' = 0.25$. This value is related to a fully inflated parachute canopy, and K' values for intermediate canopy shapes having a certain porosity are not available at this time. Therefore, in Ref. 3, it is postulated that the form factor K' for the fully inflated and the inflating parachute varies with the time T yielding for the apparent mass of the inflating canopy,

$$m_a = 0.25 \times \pi R^3\rho T \tag{12}$$

This relationship will be used in this study. It may be argued that the apparent mass, particularly for this model parachute, is negligible, but its time derivative can provide a significant contribution to the total force.

The velocity and mass derivatives are the last set of experimental nonsteady terms. Since the velocity as well as the volume and the apparent mass terms have been developed to functions of time, their derivatives can readily be obtained.

Table 1 Opening time and filling distance

V_s, fps	t_f, sec	$V_s t_f$, ft	$V_s t_f/D_0$
50	0.215	10.8	3.6
70	0.145	10.2	3.4
85	0.121	10.2	3.4

The validity of the nonsteady terms can best be checked by calculating force-time histories utilizing the averaged and generalized terms in the solution of the equation of motion. Diagrams established in this manner can then be compared with averaged force-time histories obtained from direct measurements. This method will also indicate the significance of the individual terms towards the formation of the total force.

In the preceding sections the nonsteady terms are related to the dimensionless time $T = t/t_f$. In order to establish the equation of motion, one needs to know the actual filling time of the model parachute. In Ref. 5, the filling time is defined as that period which passes while the parachute canopy inflates from its stretched out initial size to a projected area equivalent to the one which the canopy assumes under steady-state conditions. It is known, however, and the wind-tunnel experiments confirmed this, that solid cloth flat circular parachute canopies in most cases "over inflate" but that, on the other hand, the maximum force occurs in the neighborhood of the instant $t = t_f$. For the numerical opening shock calculations, it is important to have reliable values for the filling time t_f. Therefore, the film recordings were evaluated in order to obtain average filling times for each particular wind-tunnel speed. Experimental values obtained in this fashion are presented in Table 1.

The product of filling time and system velocity at the instant of snatch v_s should be constant at a given altitude as derived in Ref. 3. As seen in Table 1, this filling distance remained also in the wind-tunnel experiments practically constant. It should be mentioned, however, that the distance defined in this manner is not the actual distance which the parachute travels during its opening process but it is merely related to the opening distance as first postulated[11] and later confirmed.[9,12] In summary, the opening times shown in Table 1 appear to be valid for the solution of the equation of motion.

The compositions of the nonsteady terms are shown in Figs. 14–16. It is interesting to note that in all cases the calculated and the measured average forces at $T = 1$ agree fairly well. A strong positive contribution to the total force is provided by the time derivative of the included and ap-

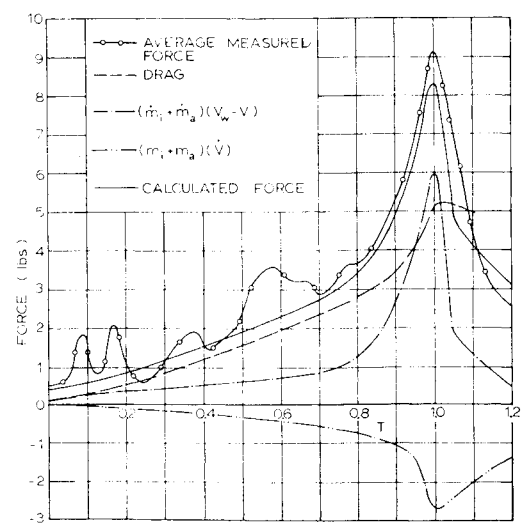

Fig. 14 Measured and calculated forces and force contributions derived from nonsteady terms at V_s = 50 fps.

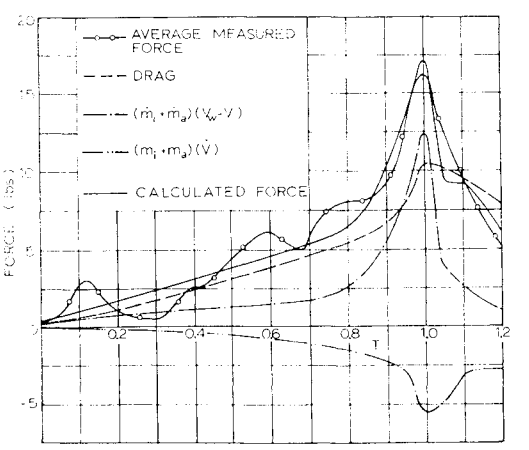

Fig. 15 Measured and calculated forces and force contributions derived from nonsteady terms at V_s = 70 fps.

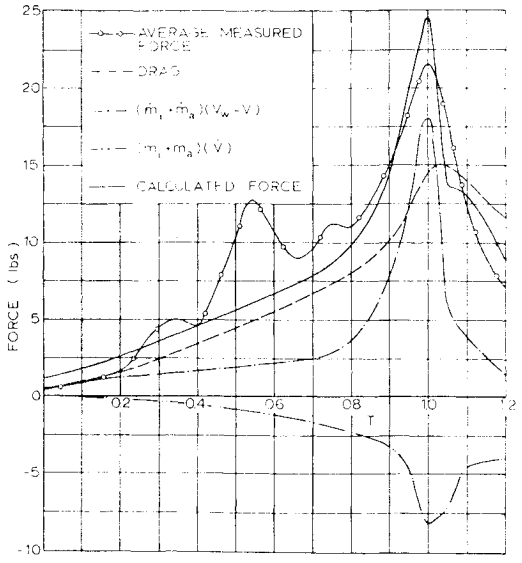

Fig. 16 Measured and calculated forces and force contributions derived from nonsteady terms at V_s = 85 fps.

parent masses, while the mass terms multiplied with the derivative of the system velocity introduce significant negative values.

The agreement between measured and calculated force-time histories in the earliest stages of inflation is not as good as the agreement near the end of the inflation. The reason for this discrepancy is probably the linearization of the area-time curve shown in Fig. 12. In this figure, it is noticed that the magnitude and slope of the measured area-time curve deviates slightly from the curve fitted function between T = 0.2–0.8. With a further refinement of the function approximating the actual area-time history, one could probably improve the agreement between calculated and measured forces in this region. However, the practical value of such a refined approximation may not be too significant, since in most cases merely the maximum forces will determine design requirements.

The composition of the unsteady terms to a total force and their fairly good agreement to the average measured force seems to justify the establishment of unique functions, at least in this experimental region.

V. Summary

The equation of motion of a parachute inflating in a wind tunnel indicates a number of nonsteady terms related to the aerodynamic drag of the inflating canopy, its included and apparent masses as well as the time derivatives of mass and velocity. Through a considerable number of wind-tunnel tests, these nonsteady terms were determined. The projected area, velocity, and included volume were reduced to unique curves covering the velocity ranges between 50 and 85 fps, representing a Reynold's number range of 0.91 $\times$ 10^6 to 1.54 $\times$ 10^6, and a ratio of included to suspended mass of 0.28. Related to the measured and averaged forces, the maximum deviations of the calculated forces amounted to -7.6 and $+11.3\%$. The discrepancies vary from a negative term at low speed to a positive term at higher speed. Also experimental errors are involved, since the instrumentation originally used produced a considerable amount of electronic hash. Improved instrumentation will probably provide better agreement. A strong influence of the included and apparent mass was noted. The nonsteady terms extracted from wind-tunnel measurements agreed in principle ith respective terms of full-size tests. The influence of model stiffness was noted, and it appears that with more flexible models, better agreement can be reached.

References

[1] Scheubel, F. N., "Der Entfaltungsvorgang des Fallschirmes," AIT 23025, 1941, Deutsche Akademie der Luftfahrtsforschung.

[2] O'Hara, F., "Notes on the Opening Behavior and the Opening Forces of Parachutes," *Journal of Royal Aeronautical Society*, Nov. 1949.

[3] "Performance of and Design Criteria for Deployable Aerodynamic Decelerators," ASD-TR-61-579, Dec. 1963, Aeronautical Systems Division, U.S. Air Force.

[4] Moog, R. D., "Mars Lander Vehicle 1 Parachute Dynamics," *Proceedings of Fifth Space Congress*, March 1968, pp. 10.2.1.–30.

[5] Berndt, R. J., "Experimental Determination of Parameters for the Calculation of Parachute Filling Times," *Jahrbuch des Wissenschaftlichen Gesellschaft fuer Luft- und Raumfahrt E. V. (WGLR)*, 1964, pp. 299–316.

[6] Berndt, R. J. and DeWeese, J. H., "Filling Time Prediction Approach for Solid Cloth Type Parachute Canopies," *AIAA Aerodynamic Deceleration Systems Conference*, AIAA, New York, Sept. 1966, pp. 17–32.

[7] Unpublished data, Air Development Center, Air Force Systems Command, Wright-Patterson Air Force Base, Ohio (related to Refs. 5 and 6).

[8] Heinrich, H. G., "The Effective Porosity of Parachute Cloth," *Zeitschrift fuer Flugwissenschaften*, Vol. 11, 1963, pp. 389–397.

[9] Ibrahim, S. K., "The Potential Flow Field and the Added Mass of the Idealized Hemispherical Parachute," *AIAA Aerodynamic Deceleration Systems Conference*, AIAA, New York, Sept. 1966, pp. 10–16.

[10] Heinrich, H. G., "Experimental Parameters in Parachute Opening Theory," *Shock and Vibration Bulletin*, No. 19, AD 9513, Research and Development Branch, Dept. of Defense, Feb. 1956.

[11] Scheubel, F. N., "Notes on the Opening Shock of a Parachute," ATI No. 34073, April 1946, Wright Air Development Center.

[12] French, K. E., "Inflation of a Parachute," *AIAA Journal*, Vol. 1, No. 11, Nov. 1963, pp. 2615–2617.